

## Experimental Demonstration of X-Ray Drive Enhancement with Rugby-Shaped Hohlräume

F. Philippe, A. Casner, T. Caillaud, O. Landoas, M. C. Monteil, and S. Liberatore  
*CEA, DAM, DIF, F-91297 Arpajon, France*

H. S. Park, P. Amendt, H. Robey, and C. Sorce  
*Lawrence Livermore National Laboratory, Livermore, California 94550, USA*

C. K. Li, F. Seguin, M. Rosenberg, and R. Petrasso  
*Plasma Science and Fusion Center, Massachusetts Institute of Technology, Cambridge, Massachusetts 02139, USA*

V. Glebov and C. Stoeckl  
*Laboratory for Laser Energetics, University of Rochester, Rochester, New York 14623, USA*  
(Received 9 November 2009; published 22 January 2010)

Rugby-shaped hohlraums have been suggested as a way to enhance x-ray drive in the indirect drive approach to inertial confinement fusion. This Letter presents an experimental comparison of rugby-shaped and cylinder hohlraums used for  $D_2$  and  $D^3He$ -filled capsules implosions on the Omega laser facility, demonstrating an increase of x-ray flux by 18% in rugby-shaped hohlraums. The highest yields to date for deuterium gas implosions in indirect drive on Omega ( $1.5 \times 10^{10}$  neutrons) were obtained, allowing for the first time the measurement of a DD burn history. Proton spectra measurements provide additional validation of the higher drive in rugby-shaped hohlraums.

DOI: [10.1103/PhysRevLett.104.035004](https://doi.org/10.1103/PhysRevLett.104.035004)

PACS numbers: 52.57.Bc, 52.50.Jm, 52.57.Fg

In the indirect drive (ID) approach to inertial confinement fusion, a fuel-filled capsule is placed at the center of a high-Z enclosure (the “hohlraum”), which converts incident laser energy to x rays that ablate the capsule and drive an implosion, compressing and heating the fuel to reach thermonuclear ignition [1]. The ignition performance margin depends on available energy delivered to the capsule; the efficiency of the conversion step is thus critical to achieve ignition on the recently commissioned National Ignition facility (NIF) [2] or on the future LaserMegaJoule (LMJ) [3]. Several approaches have been suggested to enhance the x-ray drive inside a hohlraum, such as the use of suitable mixtures of materials (“cocktails”) [4] or high-Z foams [5] for the walls, or the use of shields [6] to limit flux losses at the laser entrance holes. Recently, it was suggested to reduce the losses in the hohlraum wall by an optimization of its shape in order to reduce its area [7]. Theoretically, hohlraums with a prolate spheroid shape (“rugby-shaped hohlraums”) have a significant energetics advantage over the usual cylinders, and could be used in ignition designs with satisfying level of implosion symmetry [8]. In this Letter, we present an experimental test of the claims of x-ray drive enhancement in rugby-shaped hohlraums.

The experiment was performed on the Omega Laser Facility at the Laboratory for Laser Energetics [9], with 40 beams arranged in 3 cones on each side of the hohlraum, delivering 20 kJ in a 1 ns square pulse and smoothed by elliptical phase plates [10]. Because of the need to extract maximum laser energy and to maintain adequate laser

beam clearance in the laser entrance holes (LEHs), smoothing by spectral dispersion and polarization smoothing were not used in this experiment. The targets were scale-1 rugby-shaped and cylindrical hohlraums with the same diameter and laser entrance holes, as described in detail in the previously published design [11]. Low-convergence (50 atm gas fill) and high convergence (10 atm gas fill) capsules were imploded in both types of hohlraums to study the effects of mixing. We focus here on the low-convergence results to highlight the energetics aspects of the campaign. Some of the capsules were filled with deuterium gas with 0.026 atm of argon dopant, while the others were filled with  $D^3He$  to evaluate the areal density from the measured proton spectra [12]. A diagnostic hole is drilled on the side on the hohlraum and covered with a thin 2  $\mu\text{m}$  gold patch to allow the imaging of hot spot x-ray emission while limiting flux losses.

The x-ray flux exiting the hohlraum was measured with Dante, an array of filtered, absolutely calibrated x-ray diodes looking at one of the LEHs at  $37^\circ$  to the hohlraum axis. The radiation temperature inside the hohlraum is inferred from a Planckian fit of the lower energy channels (0–2 keV) of Dante. Although the absolute accuracy on radiation temperature is about  $\pm 5\%$ , relative shot-to-shot comparisons are more accurate ( $\pm 1\%$ ) [13]. The experimental results displayed in Fig. 1 show little dispersion for a given hohlraum shape and a clear energetic advantage for the rugby-shaped hohlraum, on the order of 18% of the x-ray flux. The faster cooling of the rugby-shaped hohlraum after the end of the laser pulse is the consequence of

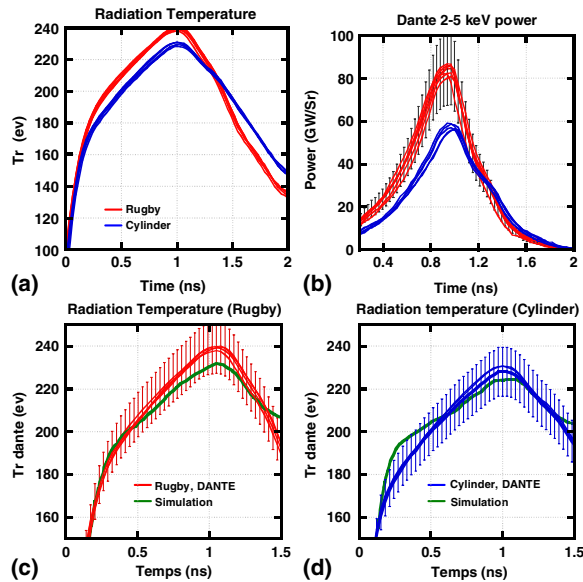


FIG. 1 (color online). (a) Drive temperature histories measured with Dante. (b) Dante (2–5 keV) x-ray power per steradian for rugby-shaped and cylinder hohlraums. (c) Comparison of simulated radiation temperature with experiment for rugby-shaped hohlraums and (d) for cylinder hohlraums.

slightly higher losses through the entrance holes at late times, based on view-factor calculations. It is worth noting that in a typical ignition design [14], the time of peak neutron production or bang time occurs near the end of the laser pulse, and this faster cooling would not be an issue. View-factor calculations and radiation hydrodynamics simulations confirm that the x-ray flux on the capsule is enhanced in the same way, as supported by proton spectral measurements. No difference in radiation temperature evolution was seen with a second diagnostic hole drilled in the hohlraum, proving the negligible x-ray losses through the gold patch.

In Fig. 1, drive measurements are compared with calculations based on integrated hohlraum radiation hydrodynamics simulations with LASNEX postprocessed to simulate the Dante view of the hohlraum wall and laser hot spots through the LEH. The calculations were performed with the measured laser power history corrected for backscatter. Time-resolved backscatter was measured on the outer laser cone with the full aperture backscatter stations [15], combining a calibrated calorimeter and a streaked spectrometer collecting the light backscattered in the focusing lens aperture. We observed 1% of backscattered energy from stimulated Brillouin scattering in the outer cones ( $58^\circ$ ) in the cylindrical hohlraum and 7% in the rugby-shaped hohlraum, whereas Raman backscatter was found to be negligible for both hohlraum types, as expected. Near backscattering imaging [16] confirmed that there was insignificant backscatter outside the aperture of the focusing lens. Since no backscatter station was available for the inner cones, their backscatter fraction was evaluated indi-

rectly by varying the amount of backscatter in the simulation to provide the best match to all experimental diagnostics including radiation drive history, x-ray core emission contours, x-ray bang time, and down-scattered proton spectra. A good agreement was found for 15% backscatter on the inner cones.

The highest energy channels of Dante provide a temporal record of 2–5 keV radiation exiting the LEH. As expected from the simulations, higher levels of x-ray flux in the gold  $M$  band are observed in the rugby-shaped hohlraum [Fig. 1(b)], consistent with the higher radiation temperature. The flux in the gold  $M$  band for rugby is close to what is predicted in simulations of a cylindrical hohlraum heated at the same temperature by increasing the laser power. This means that the use of a rugby-shaped hohlraum instead of a cylinder at the same temperature would not entail significantly more  $M$  band preheat of the capsule.

A larger amount of very hard x rays ( $\geq 10$  keV) was also observed with rugby-shaped hohlraums, both on the hard x-ray detector [17], a set of diodes sampling the spectra in the 10–50 keV range, and as a peak on neutron diagnostics shielded by 1" of lead. This is a common observation in relatively high temperature and small volume vacuum hohlraums, and could indicate fast electrons generated by two-plasmon decay near the quarter critical electron density [18]. Estimating a fraction of energy in the hot electron population under the percent level from comparison of signals with previous experiments in similar conditions, we checked in simulations that the associated preheat effects on the implosion dynamics were small compared to the effects of hohlraum geometry.

The optimized capsule design led to the highest yields to date for noncryogenic deuterium gas in indirect drive, nearly 20 times more than previously published ID  $D_2$  implosions on Omega [1]. This allowed, for the first time for deuterium in ID, the use of a full suite of neutron diagnostics, including time-of-flight detectors for determining ion temperature, primary and secondary yield, neutron emission time history (bang time and burn duration) [19,20] (Fig. 2). The only published burn-history measurements in indirect drive were conducted on Nova with DT [21]. A neutron image was also recorded for the first time in indirect drive [22], confirming the detection threshold and spatial resolution anticipated for neutron imaging systems on NIF and LMJ [23]. The DD-Ar implosion results are summarized in Table I.

In this experiment, the neutron yield in rugby-shaped hohlraums was only slightly higher than in cylindrical hohlraums. This is mostly because of the more optimal tune of the drive for cylinders, the capsule being slightly overdriven in the rugby-shaped hohlraum. As seen on the observed core shapes (Fig. 3), symmetry was also not optimal in the rugby case, because the initial design underestimated backscattering effects. In principle, the available

TABLE I. Implosion parameters deduced from the nuclear diagnostics for different hohlraums and gas types with a 50 atm fill pressure. The neutron yield-averaged ion temperature  $T_i$  is obtained by time-of-flight measurements. The compression-yield-averaged areal density  $\langle\rho R\rangle$  is deduced from the proton spectra, and  $\delta$  is the shell thickness.

Shot type	Primary yield ( $n$ )	Secondary yield (DT)	Bang time (ps)	Burn (ps)	$T_i$ (keV)	$\langle\rho R\rangle$ ( $\text{g}/\text{cm}^3$ )	$\delta$ ( $\mu\text{m}$ )
Rugby, DD	$1.29 \times 10^{10} \pm 2.00 \times 10^8$	$2.7 \times 10^7 \pm 5.92 \times 10^6$	$1932 \pm 50$	$187 \pm 20$	$3.2 \pm 0.2$	...	47
Rugby, DD	$1.51 \times 10^{10} \pm 2.16 \times 10^8$	$3.87 \times 10^7 \pm 1.89 \times 10^6$	$1873 \pm 50$	$192 \pm 20$	$3.2 \pm 0.2$	...	46
Rugby, D <sup>3</sup> He	$5.1 \times 10^8 \pm 4.0 \times 10^7$	...	$1959 \pm 100$	...	$5.0 \pm 0.2$	$6.0 \times 10^{-2}$	48
Rugby, D <sup>3</sup> He	$1.1 \times 10^9 \pm 5.84 \times 10^7$	...	$1959 \pm 100$	...	$2.3 \pm 0.2$	$8.0 \times 10^{-2}$	53
Rugby, D <sup>3</sup> He	$1.65 \times 10^9 \pm 3.99 \times 10^7$	$1.81 \times 10^6 \pm 1.53 \times 10^6$	$2025 \pm 100$	...	$2.4 \pm 0.2$	$8.0 \times 10^{-2}$	54
Cylinder, DD	$1.22 \times 10^{10} \pm 1.95 \times 10^8$	$2.52 \times 10^7 \pm 5.73 \times 10^6$	$1978 \pm 100$	...	$2.7 \pm 0.2$	...	46
Cylinder, DD	$1.37 \times 10^{10} \pm 2.06 \times 10^8$	$4.80 \times 10^7 \pm 7.90 \times 10^6$	$1812 \pm 100$	...	$2.9 \pm 0.2$	...	45
Cylinder, D <sup>3</sup> He	$1.02 \times 10^8 \pm 5.63 \times 10^7$	...	$1998 \pm 50$	$144 \pm 20$	$2.6 \pm 0.2$	$8.3 \times 10^{-2}$	48
Cylinder, D <sup>3</sup> He	$6.61 \times 10^8 \pm 4.53 \times 10^7$	...	$2112 \pm 100$	...	$2.6 \pm 0.2$	$9.1 \times 10^{-2}$	51

data set would allow one to correct the pointing and tune the capsule specifically for rugby-shaped hohlraums in an updated design, allowing better compression and higher yields.

An independent measurement of total areal densities for D<sup>3</sup>He implosions is given by proton spectra measurement using wedge range filters [12]. A multiple axis setup (up to three axes on some shots) provides an estimate of anisotropies. Areal densities deduced from the D<sup>3</sup>He implosion results [24] are summarized in Table I.

In the case of capsules in cylinder hohlraums, the implosion is very symmetric and the areal density inferred from the proton spectra is very isotropic as expected. In rugby-shaped hohlraums, the less symmetric implosion could be expected to lead to anisotropic areal density. However, proton spectra along different axes show variations in downshift that are small compared to the variation with hohlraum shape [Fig. 4(a)]. This low sensitivity of shell areal density isotropy to core shape asymmetries is related to the low-convergence ratio. Analogous observations have been reported in direct drive [25]. Note also that the measured proton yields are low along the hohlraum axis, because of magnetic fields effects [26].

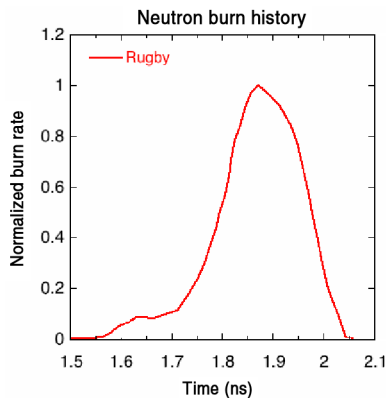


FIG. 2 (color online). Neutron burn history for a 46  $\mu\text{m}$  thick, 50 atm DD capsule in a rugby-shaped hohlraum.

The comparison will thus focus on spectra perpendicular to the hohlraum axis, where perturbations are less likely because of the near azimuthal symmetry of the laser illumination of the hohlraum walls. Images of proton emission on unfiltered CR39 track imaging detector support this choice: Anisotropies are seen in the proton flux recorded through the LEH, whereas the flux recorded through a diagnostic hole at the equator is nearly uniform.

Typically the proton spectrum consists of two features representing the early shock-flash phase (smaller downshift) and the later compressional episode. Figure 5 shows that the change in the compression part of the spectra with hohlraum shape is in good agreement with the simulations. The observed change in proton spectra downshift with decreasing capsule thickness in a rugby-shaped hohlraum is also predicted correctly, validating the ablation rate and drive on the capsule. Because of the higher drive, we find that the areal density reached by a 53  $\mu\text{m}$  capsule in the rugby-shaped hohlraum is in the same range as the areal density of a 48  $\mu\text{m}$  capsule in the cylindrical hohlraum, as predicted for a 10 eV increase of the drive with a simple  $T_R^3$  scaling of the mass ablation rate [11]. Finally this enhanced drive on capsule in rugby is confirmed by the comparison

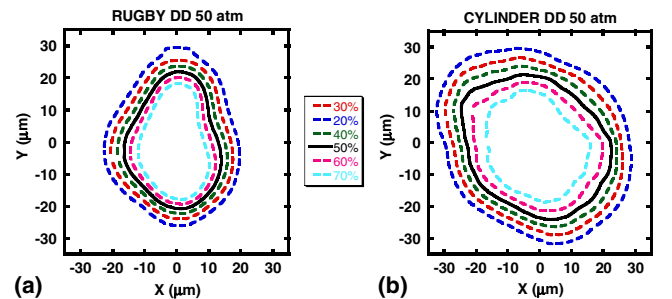


FIG. 3 (color online). X-ray emission contours of the core image at peak emission, seen through a 2  $\mu\text{m}$  gold patch, for (a) rugby-shaped hohlraum with 50 atm DD-Ar capsule and (b) cylindrical hohlraum with 50 atm DD-Ar capsule. Images are filtered at the 7  $\mu\text{m}$  instrument resolution. The hohlraum is aligned along the horizontal axis.

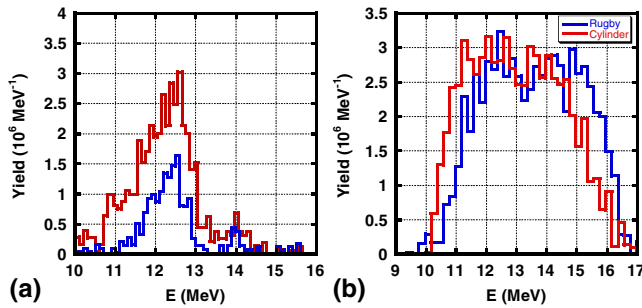


FIG. 4 (color online). (a) Comparison of proton spectra along the pole and along the equator (corrected from gold wall effect) of a  $53\ \mu\text{m}$  thick, 50 atm  $\text{D}^3\text{He}$  capsule in a rugby-shaped hohlraum. (b) Comparison of proton secondary spectra from  $46\ \mu\text{m}$  thick, 50 atm  $\text{D}_2$  capsules in rugby-shaped and cylinder hohlraums.

of secondary proton spectra of deuterium capsules in rugby-shaped and cylinder hohlraums. About 0.7 MeV less downshift is observed in the rugby case [Fig. 4(b)], also consistent with a 10 eV higher drive and more ablated mass.

Proton and neutron yields in  $\text{D}^3\text{He}$  are significantly lower in the experiment than in the simulations, by nearly an order of magnitude. This might be related to anomalies previously observed in direct-drive  $\text{D}^3\text{He}$  implosions [27], for which a theoretical explanation has been recently suggested [28].

Yield-averaged ion temperature measurements are consistent with the ratio of measured and predicted shock to compression yields: for  $\text{D}^3\text{He}$  implosions, higher ion temperature in the cylinder hohlraum is associated with a larger fraction of shock yield in the proton spectra, whereas for DD-Ar implosions, predicted in simulations to have similar shock yield fractions, ion temperature is slightly higher in the rugby-shaped hohlraums because of the stronger drive.

In conclusion, the experiment demonstrates that a significant enhancement of x-ray drive can be achieved by the use of rugby-shaped hohlraums, and that this enhancement is correctly predicted in simulations with appropriate cor-

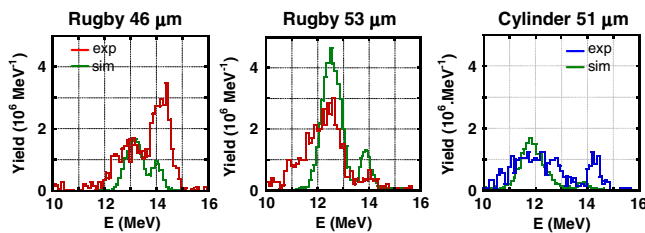


FIG. 5 (color online). Comparison of proton spectra from 50 atm  $\text{D}^3\text{He}$  capsules in rugby-shaped (two different shell thickness) and cylinder hohlraums. The simulated spectra are scaled by a factor of 0.1 for readability purposes.

rections for backscattering. It lends more confidence to extrapolations at the ignition scale. Rugby-shaped hohlraums could be used to provide either more margin at a given laser energy, higher gains, or ignition at lower energy. Even when more energy is available, operating at reduced power is an interesting option to reduce the cost of damage to optics. The drive enhancement demonstrated in this experiment is already higher than the expected benefits from other hohlraum improvement schemes, and is predicted to be even greater for an ignition scale design. Combining rugby-shaped hohlraums with cocktail materials and/or the use of shields in an advanced hohlraum design to maximize the hohlraum coupling is a promising topic for future investigations. The central remaining question for an ignition design based on the rugby concept is whether higher backscattering would partly offset its energetic benefits. A decisive answer will certainly require an experiment on a larger laser facility, such as NIF or LMJ. If significant backscatter exists at this scale, various proposals to suppress it (boron-doped walls [29], dopants in the gas fill [30]) could be investigated to reap the full benefits of rugby-shaped hohlraums.

- [1] J. Lindl *et al.*, Phys. Plasmas **11**, 339 (2004).
- [2] G. Miller *et al.*, Nucl. Fusion **44**, S228 (2004).
- [3] C. Cavallier, Plasma Phys. Controlled Fusion **47**, B389 (2005).
- [4] J. Schein *et al.*, Phys. Rev. Lett. **98**, 175003 (2007).
- [5] P. E. Young *et al.*, Phys. Rev. Lett. **101**, 035001 (2008).
- [6] D. A. Callahan *et al.*, Phys. Plasmas **13**, 056307 (2006).
- [7] P. Amendt *et al.*, Phys. Plasmas **14**, 056312 (2007).
- [8] M. Vandenboomgaerde *et al.*, Phys. Rev. Lett. **99**, 065004 (2007).
- [9] T. Boehly *et al.*, Opt. Commun. **133**, 495 (1997).
- [10] S. Regan *et al.*, J. Phys. Conf. Ser. **112**, 022077 (2008).
- [11] P. Amendt *et al.*, Phys. Plasmas **15**, 012702 (2008).
- [12] F. H. Seguin *et al.*, Rev. Sci. Instrum. **74**, 975 (2003).
- [13] C. Sorce *et al.*, Rev. Sci. Instrum. **77**, 10E518 (2006).
- [14] S. W. Haan *et al.*, Nucl. Fusion **44**, S171 (2004).
- [15] S. Regan *et al.*, Phys. Plasmas **6**, 2072 (1999).
- [16] P. Neumayer *et al.*, Rev. Sci. Instrum. **79**, 10F548 (2008).
- [17] C. Stoeckl *et al.*, Rev. Sci. Instrum. **72**, 1197 (2001).
- [18] C. Stoeckl *et al.*, Phys. Rev. Lett. **90**, 235002 (2003).
- [19] R. A. Lerche *et al.*, Rev. Sci. Instrum. **66**, 933 (1995).
- [20] C. Stoeckl *et al.*, Rev. Sci. Instrum. **73**, 3796 (2002).
- [21] M. Cable *et al.*, Phys. Rev. Lett. **73**, 2316 (1994).
- [22] T. Caillaud *et al.*, Bull. Am. Phys. Soc. **54** (2009).
- [23] L. Disdier *et al.*, Phys. Plasmas **13**, 056317 (2006).
- [24] C. Li *et al.*, Phys. Plasmas **7**, 2578 (2000).
- [25] C. K. Li *et al.*, Phys. Rev. Lett. **92**, 205001 (2004).
- [26] P. Amendt *et al.*, Bull. Am. Phys. Soc. **49**, 26 (2004).
- [27] J. R. Rygg *et al.*, Phys. Plasmas **13**, 052702 (2006).
- [28] P. Amendt *et al.* (to be published).
- [29] N. Meezan *et al.*, J. Phys. Conf. Ser. **112**, 022022 (2008).
- [30] P. Neumayer *et al.*, Phys. Plasmas **15**, 056307 (2008).